J. Iron Steel Res. Int. (2021) 28:263–271
https://doi.org/10.1007/s42243-020-00523-9

ORIGINAL PAPER

Effect of process parameters on dry centrifugal granulation of molten slag by a rotary disk atomizer

Ri-jin Cheng[1,2,3] · Hua Zhang[1,2] · Yang Li[1] · Qing Fang[1,2] · Bao Wang[1] · Hong-wei Ni[1,2]

Received: 25 December 2019 / Revised: 2 August 2020 / Accepted: 4 August 2020 / Published online: 4 January 2021

Abstract
Dry centrifugal granulation (DCG) experiments for blast furnace slag (BFS) were performed by means of a rotary disk atomizer since water quenching method can create a series of problems. The results showed that the DCG method can granulate the BFS, but the results are easily affected by the slag flow rate, disk rotating speed, disk radius, disk material and slag falling height. The granulating parameters with an excessive flow rate, low rotating speed, SiN–SiC disk, stainless steel disk and low slag falling height are detrimental to the granulation process. The most suitable parameters for granulation are a slag flow rate of 5.1×10^{-5} m^3/s, a disk rotating speed of 1500–2300 r/min, a slag falling height of 0.8 m and a smooth graphitic disk with the radius of 0.1 m. In the absence of an off-center flow, the overall best granulating effect produces round particles with mean diameter of 3.43 mm without creating slag fiber. The vitreous content of the BFS particles granulated by graphite disks is 92%, which meets the requirements of cement raw materials. The Bond work index of dry granulated BFS is 18.4 kWh/t, and the grindability of dry granulated slag and water-quenched slag is similar.

Keywords Blast furnace slag · Centrifugal granulation · Process parameter · Disk property · Grindability · Vitreous content

1 Introduction

Ironmaking has by-products such as blast furnace slag (BFS), which is produced at a rate of approximately 300 kg per ton of hot metal, and the slag has a discharging temperature of approximately 1450–1600 °C. Conventionally, BFS is treated by impinging the slag with a large volume of water to cause granulation and glassification. This treatment is mainly used for producing raw materials such as cement, aggregate and roadbed. The water quenching method can create a series of problems, including water consumption, water pollution, H_2S and SO_2 release and energy waste, and quenching necessitates a post-process for drying the slag [1–3]. To solve the above problems, the dry centrifugal granulation (DCG) method and waste heat recovery have been proposed and become a popular research topic.

It is necessary to granulate the slag before sensible heat recovery. Many researchers have studied the dry granulation of slag based on the methods of recovering sensible heat from slag and the poor thermal conductivity of slag [4–13].

Zhu et al. [14] investigated a granulation technique that combined a high-speed rotating cup with air blasting by adopting a mixture of rosin and paraffin wax as an analog of BFS and studied the effects of rotating speed, liquid viscosity, liquid flow rate and blast air flow rate on particle size, particle mass distribution and fiber mass fraction [15]. Moreover, it was found that the increase in liquid viscosity resulted in granulation mode transition under the same conditions [15]. Liu et al. [16, 17] investigated the

✉ Hua Zhang
huazhang@wust.edu.cn

✉ Hong-wei Ni
nihongwei@wust.edu.cn

[1] The State Key Laboratory of Refractories and Metallurgy, Wuhan University of Science and Technology, Wuhan 430081, Hubei, China

[2] Key Laboratory for Ferrous Metallurgy and Resources Utilization of Ministry of Education, Wuhan University of Science and Technology, Wuhan 430081, Hubei, China

[3] Technical Center, HBIS Group Hansteel Company, Handan 056001, Hebei, China

mechanism of ligament formation for molten slag granulation and the effects of the angular speed and inner depth of the rotary cup on ligament disintegration by adopting a glycerol/water mixture as a substitute for molten slag. Liu et al. [18] also investigated the solid particle diameter and size distributions of metallurgical slag with different viscosities and surface tensions by dry granulation.

Pan et al. [19] and Chang et al. [20] established physical and mathematical models of molten slag flow and heat transfer in the DCG process and discussed the influences of various factors, such as mass flow rate, temperature, molten slag surface tension, rotating speed and disk surface roughness, on the granulation process. Purwanto et al. [21] established mathematical models to predict the slag droplet diameters, glassification properties, cooling rates of slag particles and the temperature distributions within the slag particles using a rotary disk atomizer (RDA). Wang et al. [22] proposed a theoretical model to characterize the continuous free-surface film flow on the rotary disk, and the model indicated that the flow after hydraulic jump was governed primarily by the balance between Coriolis and centrifugal forces and viscous drag. The liquid film thickness distribution was mainly determined by the volume flow rate, kinematic viscosity of the molten slag and the rotating speed of disk. Purwanto et al. [23] performed dry granulation experiments for glassy slag with a rotary cup atomizer (RCA) and investigated the properties of the granulated slag, and Mizuochi et al. [1, 4] investigated the influences of the rotating speed of the RCA and the shape of the cup on the slag droplet size. Moreover, Tan et al. [24] discovered that the centrifugal granulation process was accelerated by blast air. Lin et al. [25] and Sun et al. [26] investigated the crystallization properties of molten slag under various cooling rates, based on isothermal cooling, continuous cooling and semi-rapid cooling experiments by employing single hot thermocouple technique. Ding et al. [27, 28] and Gao et al. [29] established an enthalpy-based model to analyze the phase change cooling, solidification behavior and crystallization of a molten BFS droplet and obtained an appropriate temperature of cooling air and the optimal air velocity.

Wu et al. [30] and Czisch and Fritsching [31] designed multiple groups of atomizers, performed cold experiments with water and glycerol and investigated the influences of the atomizer configuration on the granulation modes and droplet characteristics. Mizuochi and Akiyama [32] and Peng et al. [33, 34] also examined the effects of multi-shape granulation disk on the droplet size and characteristics of ligament-type granulation. It was found that the effect of rotating speed of the disk on particle size was greater than that of flow rate [34]. Tan et al. [35] discussed the effect of five kinds of disk edges on granulation characteristics and provided new insights into atomizer design towards better granulation performance of blast furnace slag. Tan et al. [36] also carried out the dry centrifugal granulation experiment and tested vitreous content, grindability and hydration activity of the granulated slag, and they identified similar grindability between the two kinds of slags. The particle size distribution and X-ray diffraction (XRD) pattern of dry granulated slag were similar to those of slag obtained from water quenching [37]; thus, the dry granulated particles could be used as a supplementary cement material with the maximum replacement reaching 60% [38].

In summary, many studies including both cold and hot experiments have been conducted on the physical properties of slag in the cooling process and the effects of different granulator shapes and rotating speeds of the RCA on slag granulation. In addition, the mechanism of slag breaking into particles and the influence of the shape of granulation disk on the granulation results have been studied by establishing the mathematical model of heat transfer and combining with experiments. In this work, the effects of granulation disk of different materials, falling height, rotating speed, mass flow rate of molten slag and disk radius on the granulation of slag were discussed. Furthermore, the Bond work index and vitreous content of obtained particles were tested.

2 Experimental

2.1 Sample

The composition of the prepared BFS sample is as follows: CaO 32.22, SiO_2 30.48, Al_2O_3 15.85 and MgO 13.79, in mass%. The melting start temperature, melting point temperature and flow temperature of the slag are 1362, 1363 and 1385 °C, respectively. The bulk density is 1400 kg/m^3, and the molten slag density is 2800 kg/m^3. The variations of viscosity and surface tension of blast furnace slag with temperature are tested using a RTW-10 rotary viscometer, which are shown in Fig. 1.

2.2 Test equipment and method

The DCG method is used to granulate the BFS, and an experimental schematic diagram of the DCG process and its apparatus is shown in Figs. 2 and 3, respectively. 2 kg of slag was added to the graphite crucible, and then, the slag was put into a $MoSi_2$ furnace for melting. After melting, the slag was preserved at that temperature for half an hour. Finally, the graphite stopper in the bottom of crucible was opened, and the BFS flowed into the center of the rotary disk, which was driven by a motor; the motor speed was controlled by an inverter. Driven by the friction of the

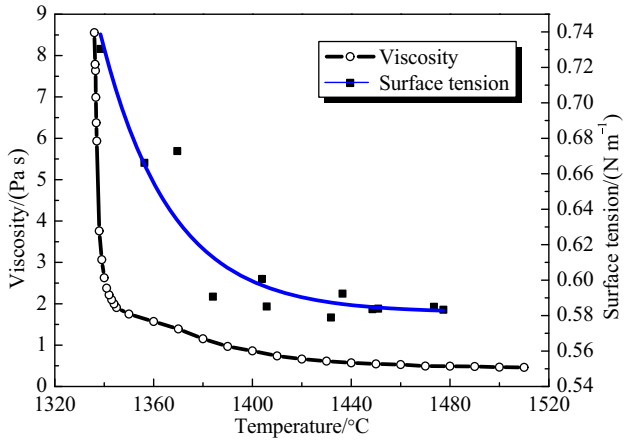

Fig. 1 Variation of viscosity and surface tension of blast furnace slag with temperature

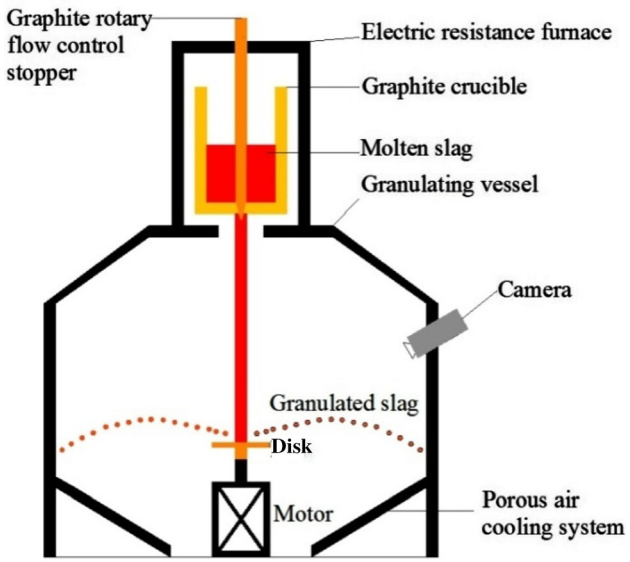

Fig. 2 Schematic diagram of experimental apparatus

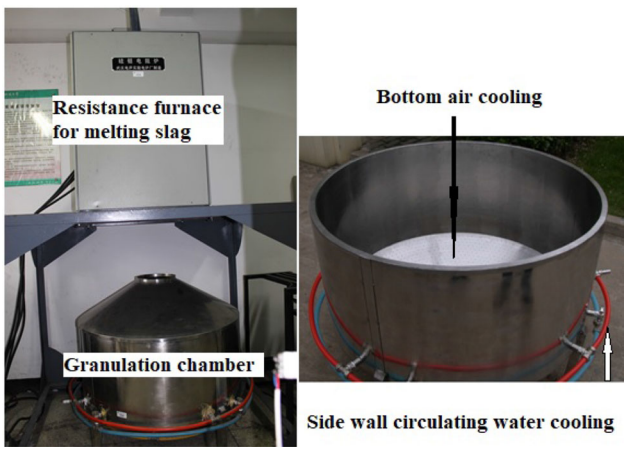

Fig. 3 Experimental apparatus of DCG process for molten slag

rotating disk, the slag was ejected from the disk due to the centrifugal force, and the ejected slag became round granules or ligaments; the ligament broke into particles by shrinkage caused by the surface tension. Finally, the slag was collected in the granulation chamber for analysis. The diameter of the granulation chamber is 1 m. The plane disks composed of different materials are shown in Fig. 4. The schematic diagrams of blast furnace slag granulation process are shown in Fig. 5. The slag collected after the test is shown in Fig. 6. The fragmentation mode of centrifugal granulation is related to the disk rotating speed and slag flow rate. According to the photographs of the experimental process shown in Fig. 5, when the rotating speed is lower than 1500 r/min, the fragmentation mode is mainly direct drop mode under the flow rate of this experiment, whereas when the rotating speed is 2300 or 2800 r/min, the fragmentation mode is mainly ligament mode.

The centrifugal granulation of BFS should not only ensure that the granulated particles are as small as possible but also ensure that the vitreous content of the granulated BFS is greater than 85%, which meets the requirements of cement raw materials. Under low flow conditions, the melt is broken into particles by dropping, and the droplet size can be calculated by Eq. (1) [32].

$$d = 4.2 \times 10^4 \cdot \left(\frac{1}{N}\right)^{0.6} \cdot \left(\frac{1}{\rho}\right)^{0.5} \cdot \left(\frac{\eta \times m}{D}\right)^{0.2} \cdot \left(\frac{\gamma}{x}\right)^{0.1} \quad (1)$$

where d is the diameter of droplets; N is the rotating speed; ρ is the density of the molten slag; η is the viscosity of the molten slag; m is the mass flow rate of the molten slag; D is the disk diameter; γ is the slag surface tension; and x represents the wetted periphery (for flat disk, $x = \pi D$).

Therefore, the diameter of the droplet is related to the disk diameter, the disk rotating speed, the slag viscosity, the slag surface tension and the slag flow rate. As can be seen in Fig. 1, within a certain temperature range, the viscosity and surface tension of the slag do not change much. Meanwhile, considering the different disk materials and slag falling heights, the test factors are shown in Table 1.

3 Results and discussion

3.1 Effects of plane disk materials on granulation results

Under the conditions of slag flow rate $Q = 5.1 \times 10^{-5}$ m^3/s, disk rotating speed $v = 2300$ r/min, slag falling height $h = 0.8$ m and plane disk radius $R = 0.10$ m, the

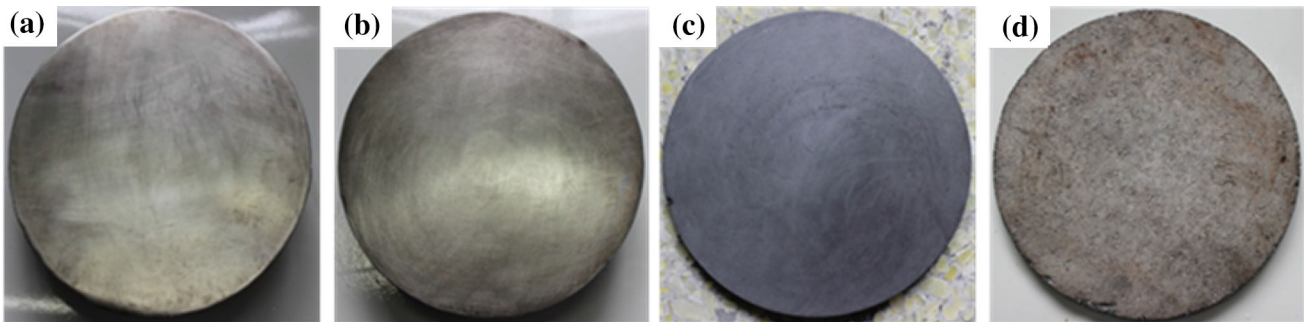

Fig. 4 Plane disks composed of different materials. **a** Stainless steel disk; **b** superalloy disk; **c** graphite disk; **d** SiN–SiC disk

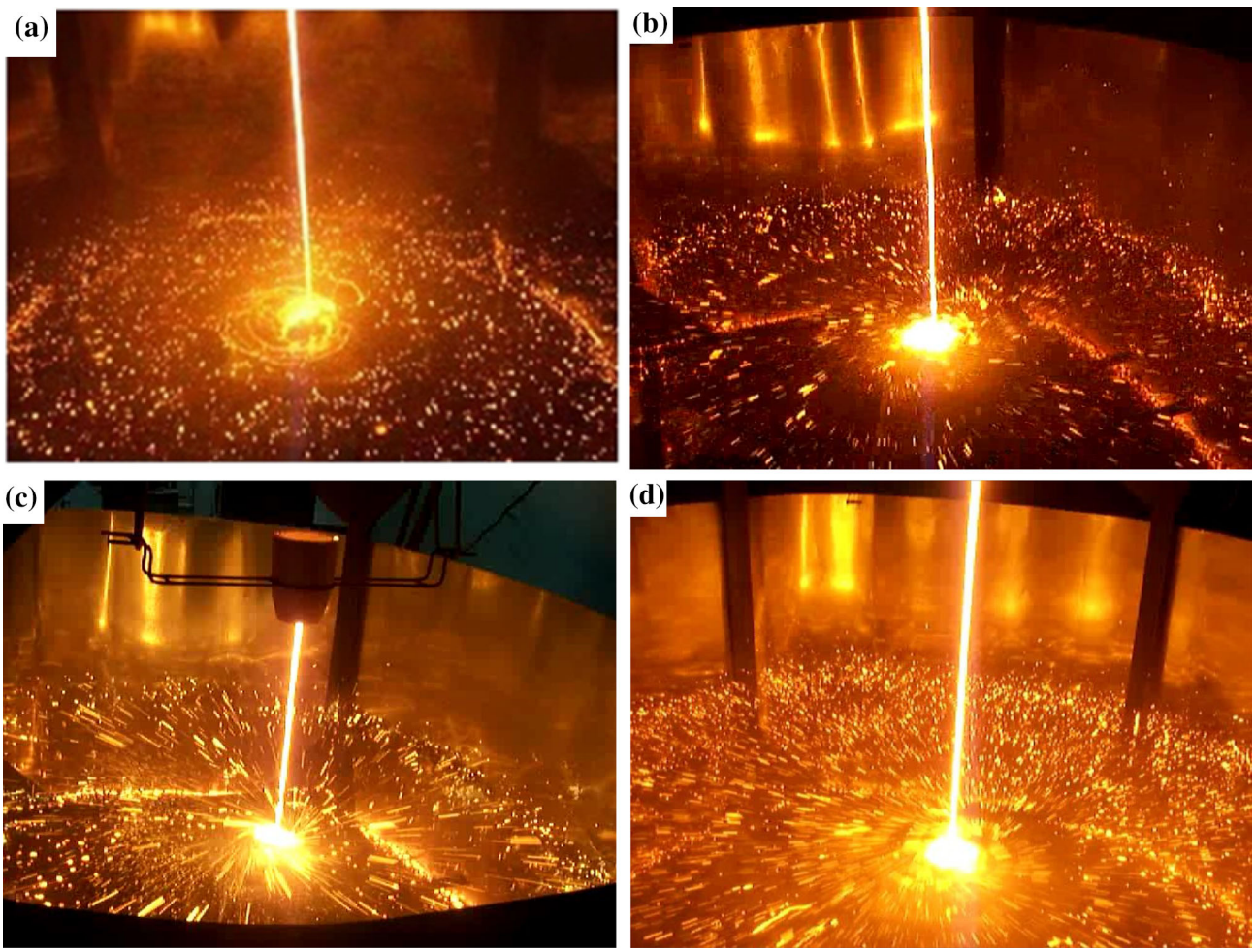

Fig. 5 Photographs of blast furnace slag granulation process with different disk rotating speeds. **a** 900 r/min; **b** 1500 r/min; **c** 2300 r/min; **d** 2800 r/min

particle size distributions of granulated slag produced by different rotating disk materials are shown in Fig. 7.

As shown in Fig. 7, the particle size distributions produced by stainless steel, superalloy and graphite disk granulation are similar, and the particle sizes are mainly concentrated in the range of 1–8 mm. Under the influence of centrifugal force, surface tension and friction resistance of the rotary disk, the slag first forms a liquid slag film, and there are circumferential and radial waves on the surface of the slag film. The instability of the slag film forces slag film to become slag ligament, and the slag ligament breaks into droplets before leaving the rotary disk [21, 39].

The stainless steel disk produced a slightly higher proportion of small granulated particles than the other disks.

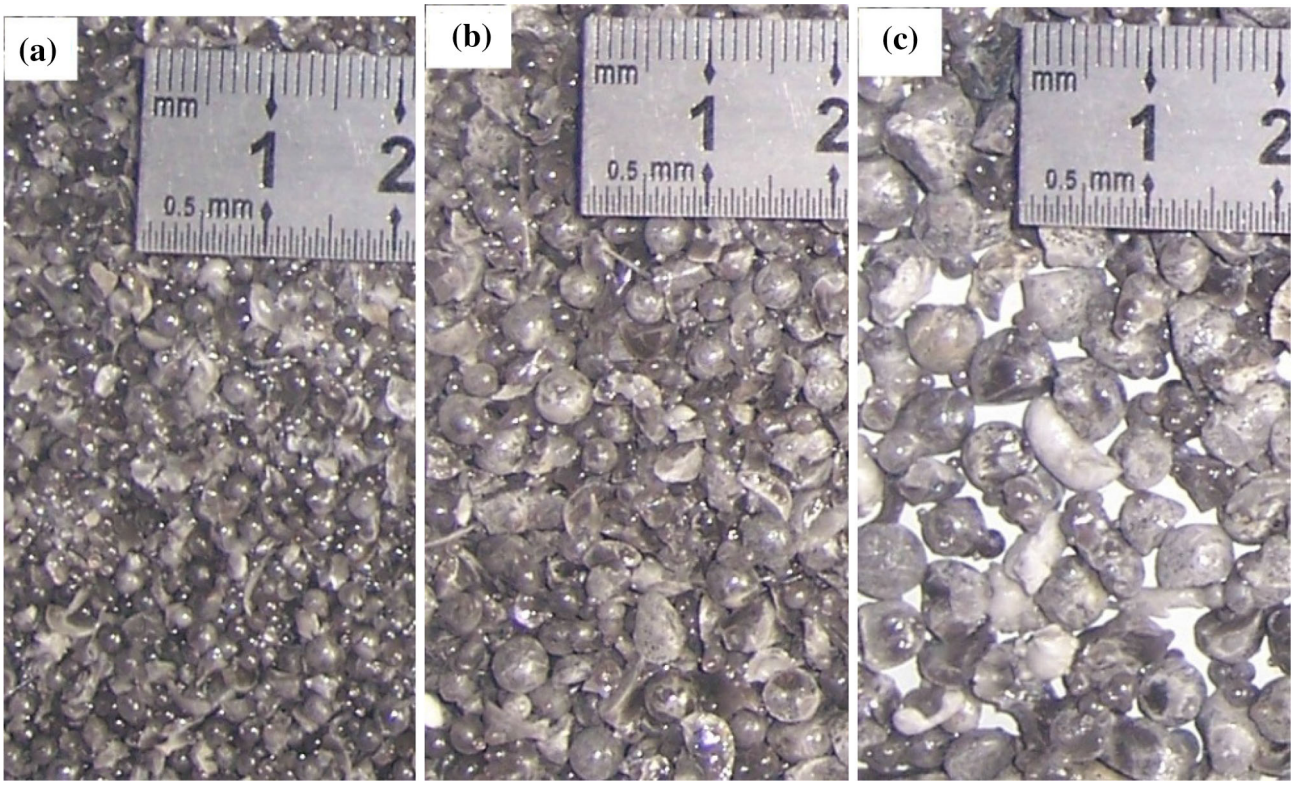

Fig. 6 Appearance of granulated BFS. **a** 0–2 mm; **b** 2–5 mm; **c** 5–8 mm

Table 1 Level of test factors

Disk material	*R*/m	*v*/(r min^{-1})	*Q*/(m^3 s^{-1})	*h*/m
Stainless steel (304)	0.15	900	2.5×10^{-5}	0.5
Superalloy (Inconel 601)	0.10	1500	3.4×10^{-5}	0.8
Graphite (w(C) > 99.99%)		2300	5.1×10^{-5}	
SiC–Si_3N_4 (20%SiC–72%Si_3N_4–8%SiO_2)		2800	1.02×10^{-4}	

w(C) Carbon content

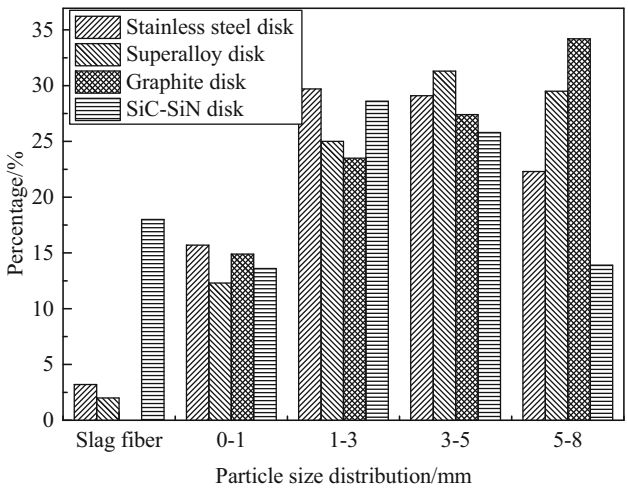

Fig. 7 Particle size distributions of slag particles produced by different rotating disks

The particle size distribution produced by the SiN–SiC disk is mainly within 5 mm, and the average slag particle diameter is 2.91 mm, which is mainly related to the surface roughness *Ra* of 100 of the SiN–SiC disk; a larger roughness is more beneficial to the granulation of slag. Slag fiber was generated by the SiN–SiC disk granulation, and the proportion of slag fiber is as high as 18%; the slag fiber adhered to the disk and cooling wall. The accumulation of slag fiber easily increased the motor load and decreased the cooling effect of the cooling wall. However, the graphite disk granulation does not produce slag fiber, because the surface roughness of the graphite disk is low (*Ra* = 3.2) and has not been greatly affected. The roughness of SiN–SiC disk is the largest, and its wettability with molten slag is the largest, followed by stainless steel disk and superalloy disk, while the roughness of graphite disk has been stable at *Ra* = 3.2, and thus, its wettability with slag is relatively small. A big wettability is favorable to the disturbance of slag, and the fine slag particles and slag fibers can be obtained. For the rotary disk with large surface roughness, the slag film is strongly disturbed, the slag

ligament is longer and finer, and the number of slag ligament increased; in the meanwhile, the heat exchange of slag ligament is stronger; thus, the slag ligament has solidified into slag fiber before leaving the rotary disk, but failed to become slag droplets [39]. In the experiment, it was found that the roughness does have a significant effect on the granulation. When using stainless steel plate to granulate slag, the surface of stainless steel plate is oxidized rapidly and the roughness of the plate increases, which results in more slag fibers when the stainless steel plate is used in the next group of experiments. In fact, more slag fibers should be avoided in the experiments.

The disk images after the granulation tests are shown in Fig. 8. Figure 8 shows that the surface roughness of the stainless steel, superalloy and SiN–SiC disks is affected by serious surface oxidation. A part of the oxide layer is attached to the surface of the disk, which results in more slag fiber in the later stage. In particular, the surface roughness of stainless steel and superalloy increased from Ra = 3.2 before dry granulation test to Ra = 6.3 after test. However, even if the graphite disk is oxidized, the gaseous oxidation products evaporate and the graphite granulation disk remains smooth as before, and the graphite disk can be used as a consumable material. In addition, the graphite disk has a lower density than the other materials; hence, the energy consumption of the granulation process is relatively small, which is also acceptable in the industry. Therefore, the graphite disk is a qualified granulation disk.

3.2 Effect of molten slag flow rate on granulation results

Under the conditions of v = 2300 r/min, h = 0.8 m, and R = 0.10 m, the particle size distributions of the granulated slag under different slag flow rates are shown in Fig. 9. Under these conditions, the quantitative relationship between the average diameter of slag and the flow rate can be expressed as $d = 269.66Q^2 - 17.295Q + 3.9578$.

As shown in Fig. 9, when the slag flow rate is large (1.02×10^{-4} m^3/s), the proportion of large slag particles is higher (the proportion of 5–8 mm slag particles is 57%),

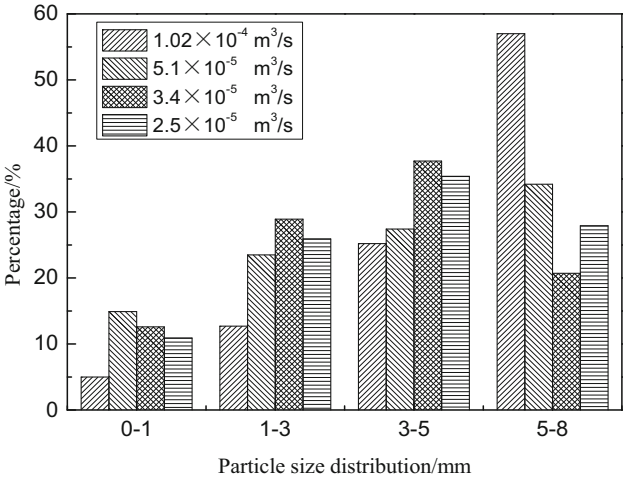

Fig. 9 Particle size distributions of slag particles under different slag flow rates

and the proportion of 0–1 mm slag particles is only 5%. As the molten slag flow rate decreases, the proportion of large particles decreases gradually, and the proportion of small slag particles increases gradually. Small slag flow is more conducive to producing small particles. When the slag flow rate is 5.1×10^{-5} m^3/s, the proportion of slag particles smaller than 3 mm is as high as 40%. When the granulation parameters are constant, the energy that can be provided to the slag granulation is constant. The larger the slag flow, the smaller the granulation energy obtained per unit mass of slag, and the overall size of the slag particles after granulation is larger. Considering the effect and efficiency of granulation, 5.1×10^{-5} m^3/s is the suitable flow rate.

3.3 Effect of disk radius on granulation results

Under the conditions of v = 2300 r/min, $Q = 5.1 \times 10^{-5}$ m^3/s, and h = 0.8 m, the particle size distributions of the granulated slag under different disk radii are shown in Fig. 10.

The radius of the disk is larger than that of the slag film, and thus, it can be seen from Fig. 10 that when the radius

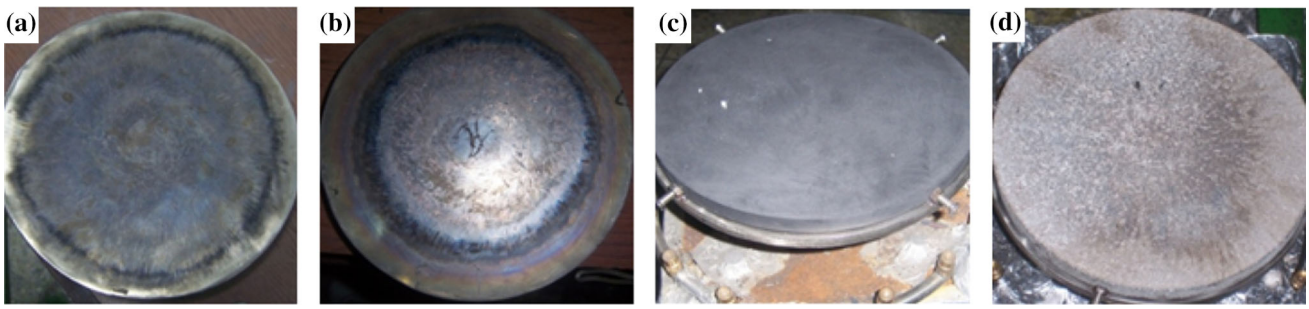

Fig. 8 Plane disks with different materials after granulation tests. **a** Stainless steel disk; **b** superalloy disk; **c** graphite disk; **d** SiN–SiC disk

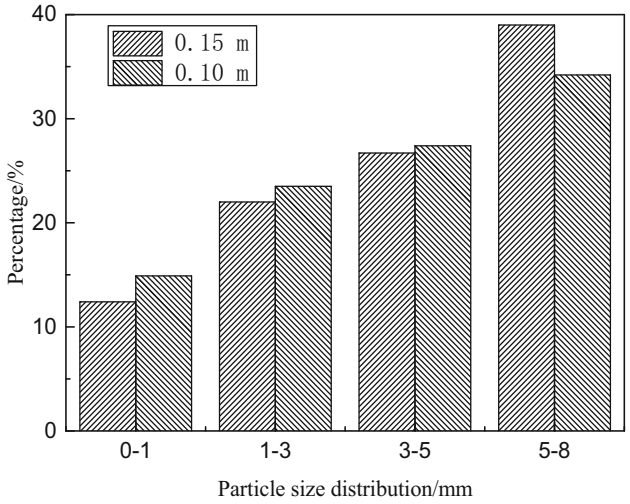

Fig. 10 Particle size distributions of slag particles under different disk radii

of the disk increases from 0.10 to 0.15 m, the particle size distribution of the slag did not change much. Under this molten slag flow rate, the 0.10 m disk meets the requirement of granulation.

3.4 Effect of slag falling height on granulation results

Under the conditions of v = 2300 r/min, $Q = 5.1 \times 10^{-5}$ m^3/s and R = 0.10 m, the particle size distributions of the granulation slag under different slag falling heights are shown in Fig. 11.

As shown in Fig. 11, when the slag falling height decreases from 0.8 to 0.5 m, the proportion of 5–8 mm slag particles increases from 34.2% to 57.8%, and the proportion of 0–3 mm slag particles decreases from 38.4% to 17.8%.

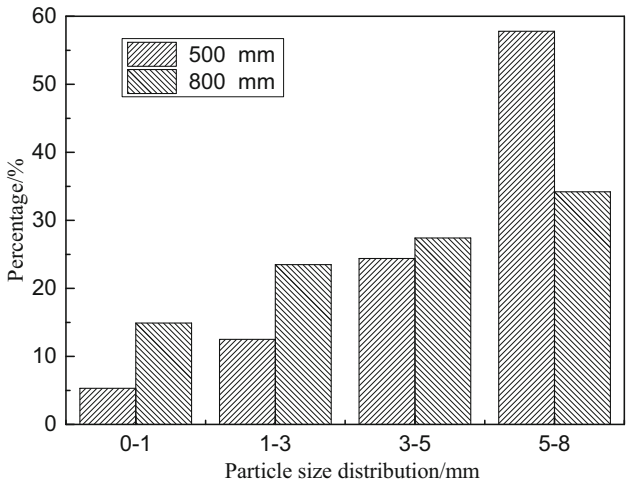

Fig. 11 Particle size distributions of slag particles under different slag falling heights

When the slag falling height increases, the slag flow falls into the rotating disk at a higher initial speed, and the kinetic energy obtained by the slag particles is larger. Moreover, the diameters of the slag particles decrease, and the granulation effect is good. However, the greater falling height may lead to a decrease in the accuracy and stability of the slag flow into the center of the disk, and the phenomenon that the slag deviates from the center of the disk during granulation is shown in Fig. 12. If the slag flow deviates from the center of the disk to a certain extent, the granulation effect is deteriorated. Therefore, the slag falling height should be appropriate.

3.5 Effect of rotating speed of disk on granulation results

When the molten slag flow rate is 3.4×10^{-5} m^3/s, the slag falling height is 0.8 m, and the graphite disk radius is 0.1 m, the particle size distributions of the granulated slag under different disk rotating speeds are shown in Fig. 13. Under these conditions, the quantitative relationship between the average particle size of slag and the rotating speed of disk can be expressed as $d = 7 \times 10^{-7}v^2 - 0.003v + 6.6513$.

As shown in Fig. 13, when the disk rotating speed is only 900 r/min, the proportion of large slag particles is higher (the proportion of 5–8 mm slag particles is 46.2%), and the proportion of 0–1 mm slag particles is only 5.9%. The proportion of large particles decreases gradually as the disk rotating speed increases, and the proportion of small slag particles increases gradually; hence, a larger disk rotating speed is more favorable for obtaining smaller slag particles. When the disk rotating speed is greater than 2300 r/min, subsequent increases in the rotating speed have little positive influence on the particle size distribution. The disturbance of slag increases at high speed, which is beneficial to slag granulation. However, when the rotating speed of disk is large, the heat transfer of slag is strong, and

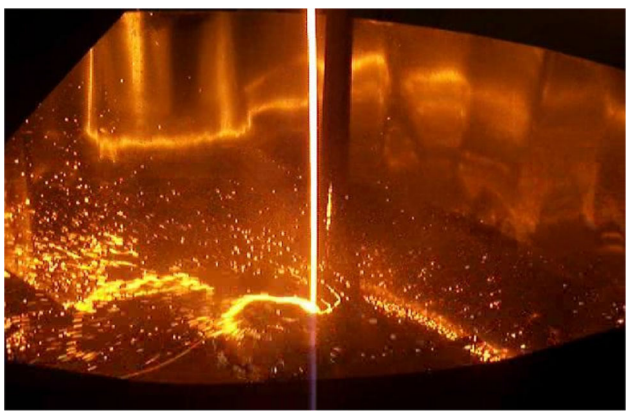

Fig. 12 Photograph of slag deviated from center of disk during granulation

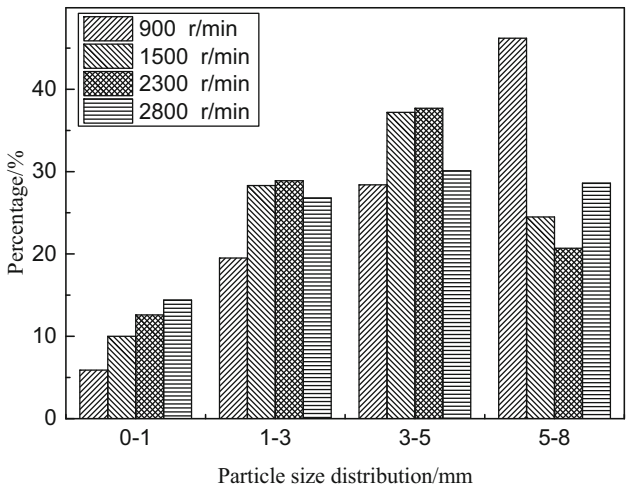

Fig. 13 Particle size distributions of slag particles under different disk rotating speeds

the viscosity and surface tension of slag increase; thus, it is not conducive to producing finer slag film and slag ligament. At the same time, if the rotating speed is too high, the energy consumption of slag granulation will increase, and subsequently, the recovery rate of sensible heat of slag will be reduced. Therefore, the proper speed is favorable for slag granulation.

3.6 Uncertainty analysis of experiments

There may be several sources of experimental errors. The first is that the slag columnar flow needs to be kept near the center of the granulation disk during the experiment, and there is no off-center flow, as shown in Fig. 12. The second is the flow control. In this experiment, the rotating angle of the rotating handle with angle scale is used to control the stopper (Fig. 2); therefore, the accuracy is easy to control. The third is that the tundish needs to be baked to 1300 °C, and it should be placed at the bottom of the high-temperature furnace before the stopper is opened. The connection operation should be rapid and timely to prevent the tundish from waiting too long to affect the slag temperature. The fourth is the roughness of the granulation disk. The granulation disk made of alloy and stainless steel has a larger roughness change after being used for many times. It needs to be polished in time before it can be used in the next experiment.

3.7 Vitreous content and grindability of granulated slag

Under the conditions of $Q = 5.1 \times 10^{-5}$ m^3/s, $v = 2300$ r/min, $h = 0.8$ m and $R = 0.10$ m, the slag particles granulated by two typical materials, stainless steel and graphite, were analyzed by XRD. Before XRD test, 200 g of granulated slag particles containing different particle sizes is taken for grinding, and the size of the crushed powder should be smaller than 75 μm. The vitreous content for the slag particles analyzed by XRD examination is shown in Fig. 14.

As shown in Fig. 14, the amorphous structures of BFS particles granulated by stainless steel disk and graphite disk indicate that the dry granulated slag particles have high glass contents. According to the determination method in GB/T 18046-2008, the vitreous content of BFS particles granulated by stainless steel disk and graphite disk is 88.07% and 92.00%, respectively, and it meets the requirements of cement raw materials. In combination with the previous analysis results, the dry granulation of BFS achieves vitreous contents > 85% in all kinds of conditions.

The Bond work index (BWI) values of the water-quenched slag and dry granulated slags in this granulation experiment were measured.

The BWI of dry granulated BFS is 18.4 kWh/t, which is slightly less than the BWI of water-quenched slag (21.2 kWh/t). This indicates that the grindability of the dry granulated slag and water-quenched slag is similar. The use of dry granulated slag instead of water-quenched slag as cement raw materials will not increase the grinding energy consumption of the raw materials in cement production.

4 Conclusions

1. The DCG method can granulate BFS, and the granulation effect is influenced by the slag flow rate, disk rotating speed, disk radius, disk material and slag falling height.
2. The disk material has a greater effect on the slag granulation than the other tested factors. When the

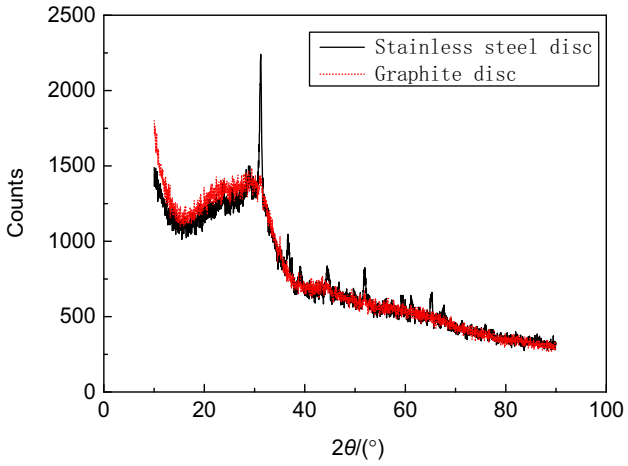

Fig. 14 XRD test results of centrifugally granulated slag

SiN–SiC disk with high roughness is used for granulation, fine slag particles with an average diameter of 2.91 mm can be obtained, while the proportion of slag fiber of 18% can cause negative effects on the granulation process. The polished stainless steel and superalloy disks can also produce good granulation effects, but these disks also produce 3.2% and 2.0% of slag fiber, respectively. The smooth graphite disk is the most suitable disk for granulation among the tested disks: The overall average particle diameter produced by the graphite disk is 3.43 mm, and no slag fiber is produced during the granulation process.

3. When the slag is not covering the disk, increasing the radius of the disk has little effect on the particle size distribution. By increasing the falling height of the molten slag, the kinetic energy of the slag particles increases, and the average diameter of the slag particles decreases.
4. When the slag flow rate decreases, the proportion of small slag particles increases gradually. When the slag flow rate is less than 5.1×10^{-5} m^3/s, the overall average particle diameter is less than 4 mm.
5. As the rotating speed of the disk increases, the proportion of small particles increases gradually, and a larger rotating speed of the disk is more favorable for obtaining smaller particles. When the rotating speed of the disk increases above 2300 r/min, the rotating speed has little effect on the particle size distribution.
6. The vitreous contents of BFS particles granulated by stainless steel disk and graphite disk are 88.07% and 92.00%, respectively, which meets the requirements of cement raw materials. The BWI of dry granulated BFS is 18.4 kWh/t, and the grindability of dry granulated slag and water-quenched slag is similar.

Acknowledgements This work was financially supported by the National Key Research and Development Program of China (2018YFC1900602) and the Open Youth Fund of the State key Laboratory of Refractories and Metallurgy, Wuhan University of Science and Technology (2018QN03).

References

[1] T. Mizuochi, T. Akiyama, T. Shimada, E. Kasai, J.I. Yaji, ISIJ Int. 41 (2001) 1423–1428.
[2] Y.Q. Sun, Z.T. Zhang, L.L. Liu, X.D. Wang, Energies 7 (2014) 1673–1684.
[3] H. Wang, J.J. Wu, X. Zhu, Q. Liao, L. Zhao, Appl. Energy 171 (2016) 314–324.
[4] T. Akiyama, T. Mizuochi, J.I. Yagi, H. Nogami, Steel Res. Int. 75 (2004) 122–127.
[5] H. Purwanto, T. Akiyama, Int. J. Hydrogen Energy 31 (2006) 491–495.
[6] J. Ding, Y.R. Wang, R. Gu, W.L. Wang, J.F. Lu, Appl. Energy 250 (2019) 1270–1279.
[7] H. Purwanto, E. Kasai, T. Akiyama, ISIJ Int. 50 (2010) 1319–1325.
[8] M. Cooksey, A. Guiraud, B. Kuan, Y.H. Pan, J. Sustain. Metall. 5 (2019) 181–194
[9] Y.Q. Sun, Z.T. Zhang, Metall. Mater. Trans. E 3 (2016) 114–122.
[10] Y.Q. Sun, Z.T. Zhang, L.L. Liu, X.D. Wang, Energies 8 (2015) 1917–1935.
[11] T. Shimada,V. Kochura, T. Akiyama, E. Kasai, J.I. Yagi, ISIJ Int. 41 (2001) 111–115.
[12] T.D. Hadley, Y.H. Pan, K.S. Lim, J. Orellana, Int. J. Miner. Process. 142 (2015) 91–100.
[13] N. Wang, H. Peng, X. Ling, J.Q. Kang, M.H. Xu, Energy Procedia 105 (2017) 622–627.
[14] X. Zhu, H. Zhang, Y. Tan, H. Wang, Q. Liao, Appl. Therm. Eng. 88 (2015) 157–164.
[15] J.J. Wu, H. Wang, X. Zhu, Q. Liao, B. Ding, Appl. Therm. Eng. 89 (2015) 494–504.
[16] J.X. Liu, Q.B. Yu, P. Li, W.Y. Du, Appl. Therm. Eng. 40 (2012) 351–357.
[17] J.X. Liu, Q.B. Yu, W.J. Duan, Q. Qin, Appl. Therm. Eng. 73 (2014) 888–893.
[18] J.X. Liu, Q.B. Yu, Z.L. Zuo, W.J. Duan, Z.C. Han, Q. Qin, F. Yang, Appl. Therm. Eng. 103 (2016) 1112–1118.
[19] Y.H. Pan, P. Witt, D.S. Xie, in: 7th Int. Conference on CFD in the Minerals and Process Industries, CSIRO, Melbourne, Australia, 2009, pp. 1–6.
[20] Q.M. Chang, X.W. Li, H.W. Ni, W.Y. Zhu, C.G. Pan, S.D. Hu, ISIJ Int. 55 (2015) 1361–1366.
[21] H. Purwanto, T. Mizuochi, T. Akiyama, Mater. Trans. 46 (2005) 1324–1330.
[22] D.X. Wang, X. Ling, H. Peng, Appl. Therm. Eng. 63 (2014) 387–395.
[23] H. Purwanto, T. Mizuochi, H. Tobo, M. Takagi, T. Akiyama, Mater. Trans. 45 (2004) 3286–3290.
[24] Y. Tan, X. Zhu, X.Y. He, B. Ding, H. Wang, Q. Liao, H. Li, Powder Technol. 323 (2018) 176–185.
[25] B. Lin, H. Wang, X. Zhu, Q. Liao, B. Ding, Appl. Therm. Eng. 96 (2016) 432–440.
[26] Y.Q. Sun, H.W. Shen, H. Wang, X.D. Wang, Z.T. Zhang, Energy 76 (2014) 761–767.
[27] B. Ding, X. Zhu, H. Wang, X.Y. He, Y. Tan, Int. J. Heat Mass Transfer 118 (2018) 471–479.
[28] X. Zhu, B. Ding, H. Wang, X.Y. He, Y. Tan, Q. Liao, Appl. Therm. Eng. 130 (2018) 1033–1043.
[29] J. Gao, Y.H. Feng, D.L. Feng, Z. Zhang, X.X. Zhang, Int. J. Heat Mass Transfer 146 (2020) 118888.
[30] J.J. Wu, H. Wang, X. Zhu, Q. Liao, K. Li, Appl. Therm. Eng. 111 (2017) 1557–1564.
[31] C. Czisch, U. Fritsching, Mater. Sci. Eng. A 477 (2008) 21–25.
[32] T. Mizuochi, T. Akiyama, ISIJ Int. 43 (2003) 1469–1471.
[33] H. Peng, X.K. Shan, X. Ling, D.X. Wang, J. Li, Appl. Therm. Eng. 128 (2018) 1565–1578.
[34] H. Peng, X.K. Shan, X. Ling, D.X. Wang, J. Li, Results Phys. 11 (2018) 385–393.
[35] Y. Tan, H. Wang, X. Zhu, Y.W. Lv, X.Y. He, Q. Liao, Appl. Therm. Eng. 159 (2019) 113977.
[36] Y. Tan, X. Zhu, H. Wang, X.Y. He, B. Ding, Q. Liao, Appl. Therm. Eng. 142 (2018) 683–694.
[37] J.X. Liu, Q.B. Yu, Z.L. Zuo, F. Yang, W.J. Duan, Q. Qin, Constr. Build. Mater. 131 (2017) 381–387.
[38] J.X. Liu, Q.B. Yu, Z.L. Zuo, F. Yang, Z.C. Han, Q. Qin, Cement Concr. Compos. 95 (2019) 19–24.
[39] J.J. Wu, H. Wang, X. Zhu, Q. Liao, J. Li, L. Lin, CIESC Journal 66 (2015) 2474–2480.